Multistage chemical bath deposition of thick film cadmium sulfide for CdS/CdTe X-ray detector

H. SHAMS [1], H. ABOU GABAL [1], M. SOLIMAN [2], S. EBRAHIM [2], S. AGAMY[1]

[1-] Nuclear and Radiation Engineering Department, Faculty of Engineering, Alexandria University, Egypt.

[2-] Materials Science Department, Institute of Graduate Studies and Research, Alexandria University, Egypt.

Abstract

Many methods are used to measure X-ray flux generated by modern X-ray machines. The most common method utilized for monitoring X-ray dose is technically complex and expensive. In this work multilayer of cadmium sulfide (CdS) using chemical bath deposition (CBD) were carried out to deposit thick layer optimum thickness to produce CdS/CdTe junction x-ray detector. The effects of the deposition time, cadmium chloride heat treatment, the ammonia and thiourea concentration on CdS layers were controlled and investigated through scanning electron microscope (SEM), energy dispersive x-ray analysis (EDXA), X-ray diffraction (XRD), and ultraviolet (UV)-visible spectroscopy. The XRD analysis showed that the CdS films have highly oriented crystallites with the classical hexagonal structure (wurtzite type) and the main six diffraction peaks. The relatively stronger and narrow peak of CdS film obtained with 6 stages along (002) plane indicated that the film is highly oriented along the c-axis. The band gap E_g can be extrapolated to be 2.41 eV. It was observed that the maximum and the minimum amplitudes of the pulse formed due to exposed FTO/CdS/CdTe/Mo detector to X-ray of 33 keV and 1mA intensity are 0.732 and -0.405 V and consequently the total output amplitude is 1.137 V.

Keywords: CdTe; CdS; Thin film; X-ray; Detector

1. Introduction

Deposition of thin chalcogenide films by vacuum evaporation, sputtering and chemical methods are well known and interested in the fabrication of solar selective coatings, solar cell, photoconductors, sensors and detectors [1]. CBD technique is recognized to be a relatively simple, low cost and scalable for the deposition of high quality CdS thin film required by the solar cell industry. CBD has been used in the deposition of CdS semiconductor thin film. CdS as a n-type semiconductor has been used as a window and buffer layer in the fabrication of efficient thin film solar cells based on CdTe or Cu (In,Ga) SeS [2]. Wagner et al prepared CuInSe/CdS heterojunction photovoltaic detector for

spectroscopy in the visible and near infrared regions. They found that the spectral dependence of the quantum efficiency was bias dependent for diodes with appreciable insulating layers of reverse bias ≥2 V or at zero bias for diodes with no insulating layer [3]. Tomita et al fabricated CdS/CdTe heterojunction devices by radio frequency sputter deposition method to be used for x-ray imaging sensors. It was noted that an x-ray imaging camera tube consisting of CdS/CdTe heterojunction photoconductive target had three times larger responses to x-rays than the conventional PbO x-ray tube [4]. Murphy et al fabricated thin film diode based on CdTe with a diameter of up to 3.5 mm to function effectively as single-event charged particle detectors and CdTe was deposited using close-space sublimation. They found that the individual alpha particles were detected with an intrinsic efficiency of >80%, while the junctions were insensitive to gamma rays [5]. Kang et al used Monte Carlo simulations to employ deeply penetrating mega-voltage x-rays delivered with linear accelerator and specified the quantity of x-ray exposed using thin film CdS/CdTe then they verified the measurements using fabricated prototype CdS/CdTe solar cells, which fabricated by the sequential deposition of SnO_2, CdS, CdTe, and aback contact layer. The fabricated prototype has shown remarkable accurate readings of the x-ray beam intensity compared to the MC simulations [6].

There are other different methods have been applied to deposit CdS thin films such as electrodeposition, spray pyrolysis, molecular beam epitaxy, metal organic chemical vapor deposition, successive ionic layer adsorption and reaction, physical vapor deposition and sputtering [7-14]. However, CBD cannot use in the ionizing radiation sensing applications in which thicker and high quality CdS films are required. This is due to the following two reasons. First, the formation of a saturate CdS layer is between 0.05 and 0.2 μm and duplex layer is formed by longer of the deposition time. The duplex layer consists of very adherent inner layer and a less adherent outer layer. Second, the heterogeneous reaction on the substrate surface (increasing the CdS thickness), homogenous reaction in the bulk of the solution (increasing the CdS concentration in the solution) is presented[15].The main target to this work is to investigate the effect of different deposition parameters of CdS, such as the deposition time, molar concentrations of thiourea and ammonia on the surface morphology, the chemical composition, thickness and the optical property. The multistage deposition of CdS thick film is carried out onto the FTO substrate to overcome the limited thickness. In addition, the performance of thick CdS/CdTe heterojunction as X-ray detector is studied.

2. Materials and Methods

2.1 Materials

Cadmium acetate dihydrate(99%, MW=266.52 g/mole)was obtained from Merck. Ammonium acetate(98%, MW= 77.08 g/mole)was purchased from Carlo Erba. Ammonia (25%, MW 17.03 g/mole)was received from Chem. Thiourea(99% MW=76.12g/mole)was obtained from Loba Chemi. Cadmium chloride pentahydrate was obtained from Sigma Aldrich. Fluorine doped tin oxide (FTO) coated glass slide with sheet resistance of 7 Ohm/sq was bought from Sigma Aldrich.

2.2 Preparation of thick film of CdS

CdS films were deposited on FTO substrate using a heated alkaline solution of cadmium acetate dihydrate as the Cd^{2+} source, thiourea as the S^{2-} source, ammonium acetate serving as a buffer and ammonia as a complexing agent. CdS films, were prepared using different molar concentrations of thiourea (0.06 - 0.09M) and ammonia (8-11-14M) with 0.03 M cadmium acetate dihydrate and 1M ammonium acetate [16]. The FTO glass substrate was immersed in a solution of cadmium acetate dihydrate, the ammonium acetate and the ammonia and heated with stirring at88 ^{o}C through 30minutes. The thiourea solution was added dropwise in four aliquots every 10 minutes. After the CdS deposition, the substrate was removed from the bath and placed in warm deionized water. Finally, the substrate was sonicated for about 2 minutes to remove loosely adherent CdS particulates. The treatment of CdS film was achieved by dropping1 N solution of $CdCl_2$ in methanol and the films was heated at 350 ^{o}C for 15 minutes. The deposition time was varied from 2 to 4 hours. Multistage deposition of CdS thin films was achieved to control the thickness of the films. Six successive layers were deposited by the same conditions.

2.3 Fabrication of CdS/CdTe X-ray detector

CdTe was electrodeposited onto the prepared CdS/FTO substrates. CdTe was deposited using potentiostate Gamry750G using a two-electrode cell. The system consisting of CdS/FTO working electrode as a cathode and a graphite electrode as an anode immersed in an electrolyte. The electrolyte solution consists of cadmium sulfate $3.8x10^{-2}$M solution, $4.2x10^{-2}$ M of $CdCl_2$ and 10^{-3}M of TeO_2. The TeO_2 solution was prepared by dissolving 0.032 gm of TeO_2 in 2ml of dilute sulfuric acid and then this solution was added to 200ml of deionized water. The produced heterojunction was treated again with 1 N $CdCl_2$ at 350^{o}C for 15 min. and was cleaned with distilled water. The cyclic voltammetry was used to provide the optimum applied voltage for CdTe deposition onto CdS/FTO glass

substrate, where -1.2 V was found suitable for CdTe film deposition. By growing CdTe layer onto CdS/FTO at constant voltage a homogeneous good distribution layer was established.

Mo metal as a back contact was deposited on CdTe/CdS/FTO hetero junction samples by DC magnetron sputtering system (HUMMER 8.1). The CdTe/CdS/FTO hetero junction samples were subsequently put into the vacuum chamber and placed at a distance of 10 cm from the Mo target. The vacuum chamber was initially evacuated to a base pressure of8×10^{-5}kPa. Then pure argon flow of 0.094 L^2/min was introduced into the chamber to keep the pressure during the film deposition at a value around 1.9 10^{-4}kPa. The power supply was then turned on and adjusted at 60 W. The schematic diagram of the fabricated detector with different layers is shown in Figure (1).

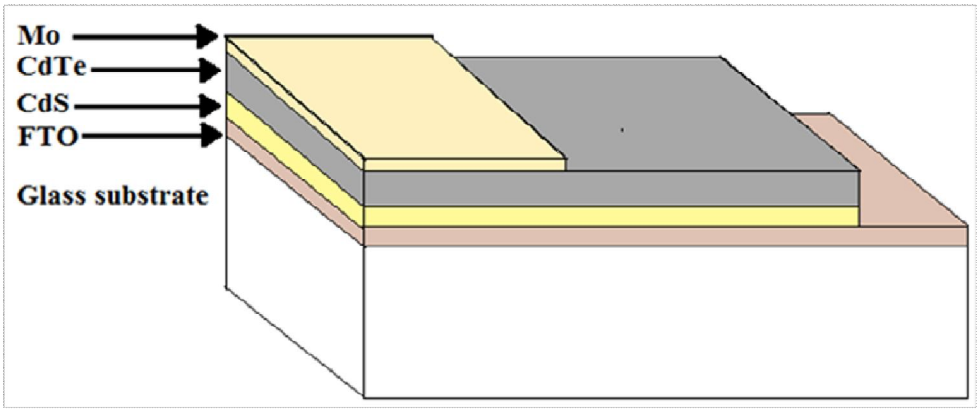


Figure (1) The structure of the fabricated x-ray detector.

2.4Characterization techniques

To characterize the deposited CdS films, a scanning electron microscopy QUANTA FEG250 was used to observe the surface morphology and measure the film thickness. The chemical compositions of the films were determined with an Energy dispersive x-ray spectrometer QUANTA FEG250. The crystalline structure was studied by means of x-ray diffraction using (x-ray 7000 Shimadzu-Japan) at room temperature. The Bragge angle (2θ) in the range from 5 to 50 degrees was measured. The x-ray source was Cu target generated at 30 KV and 30 mA with scan speed 4 deg/min. The electronic absorption spectra were obtained using UV-Visible spectrophotometer (Evolution 600 double beams scanning UV-visible spectrophotometer, Thermo scientific, USA) in the range of 200-800nm.

2.5 Performance measurement of CdS/CdTe X-ray detector

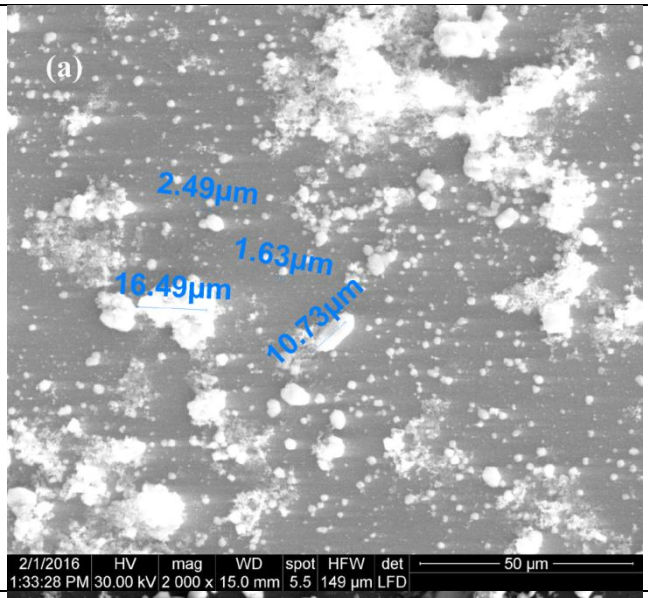
X-ray generator Geratogram Roentgen instrument (Germany, 1987) was used to produce an X-ray adjustable energy range of 21 to 42 keV and with an emission current adjustable range of 0.05 to 1 mA with local dose rate at a distance of 0.1m from the touchable surface of the device is ≤ 5μSv.The perpendicular X-ray was incident onto the fabricated CdS/CdTe detectors. The output of four stacked detectors in series was connected to computerized oscilloscopeDS03064 Kit V to read the output signal.

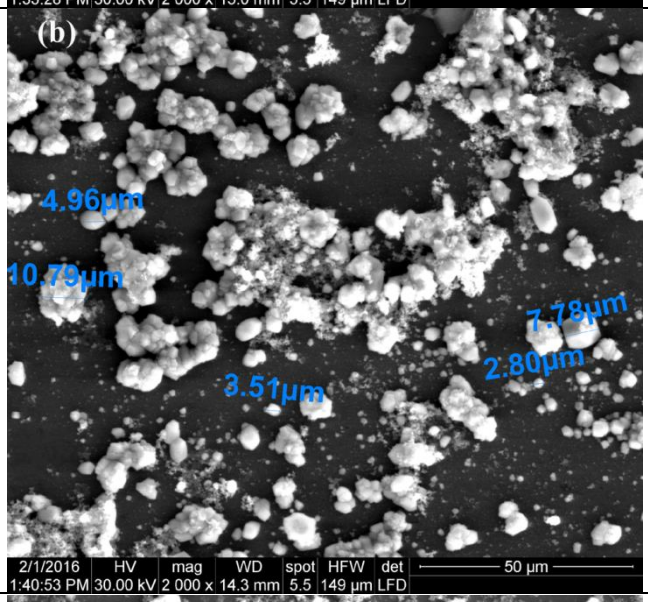
3. Results and Discussion

3.1 Surface Morphology and Composition Analysis of CdS thick film

3.1.1Effect of deposition time

The influence of the deposition time on the morphology of the CdS films is shown in Figure (2). The SEM micrographs show that the formed CdS films have a good adherence to the FTO substrate with a few pinholes at 4 hrs deposition time. Moreover, the FTO surface is covered with spherical grains and their sizes decrease from 16 to 1.9 μm and their densities increase with a long time of deposition. The small particles of CdS are accumulated continuously and covered the entire surface of the substrate to produce a homogeneous CdS layer. This indicates that the homogeneity of the CdS film is better with4 hrs deposition time. This result is similar to that recorded by Fouad et al [18]. However, we extend the deposition time for 4 hrs to enhance the adhesion and to produce homogeneous and smooth surface. The EDX analyses indicate the atomic percents of S/Cd are37.16/62.84,21.45/78.55 and 45.7/54.3 correspond to 2.0,3.0 and 4.0 hrs, respectively. It is noticed that at 4 hrs depositions time, the S/Cd ratio is more stoichiometry than 2 and 3 hrs. This is attributed to the longer time of deposition increasing the number of collisions and the probability of formation of CdS compound [17].





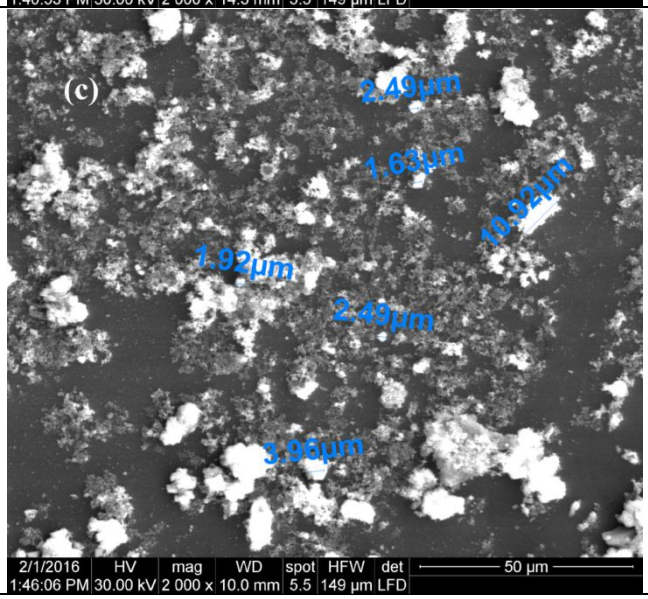


Figure (2) SEM micrographs of CdS films deposited with different deposition times: (a)2hours, (b)3hours, (c)4hours.

3.1.2Effect of ammonia concentration

The SEM micrographs of the surface morphology of the CdS films deposited with different ammonia concentrations (14,11 and 8M) are illustrated in Figure (3). The micrographs reveal that the CdS films are smooth, homogeneous with few cracks and the good distribution of the granules at low concentration is observed [18].The EDX results of the CdS films prepared with the different ammonium hydroxide concentrations indicate that the atomic percent of S/Cd are 45.7/54.3, 42.71/57.29 and 52.65/47.35 at ammonia concentration of 14.0, 11.0 and 8.0 M, respectively which mean a better stoichiometric ratioat low ammonia concentration is obtained. Hasnetet al reported that the quantitative results of pure CdS thin film from EDX analysis yieldeda Cd to S ratio equal to 1.09 [19-20].

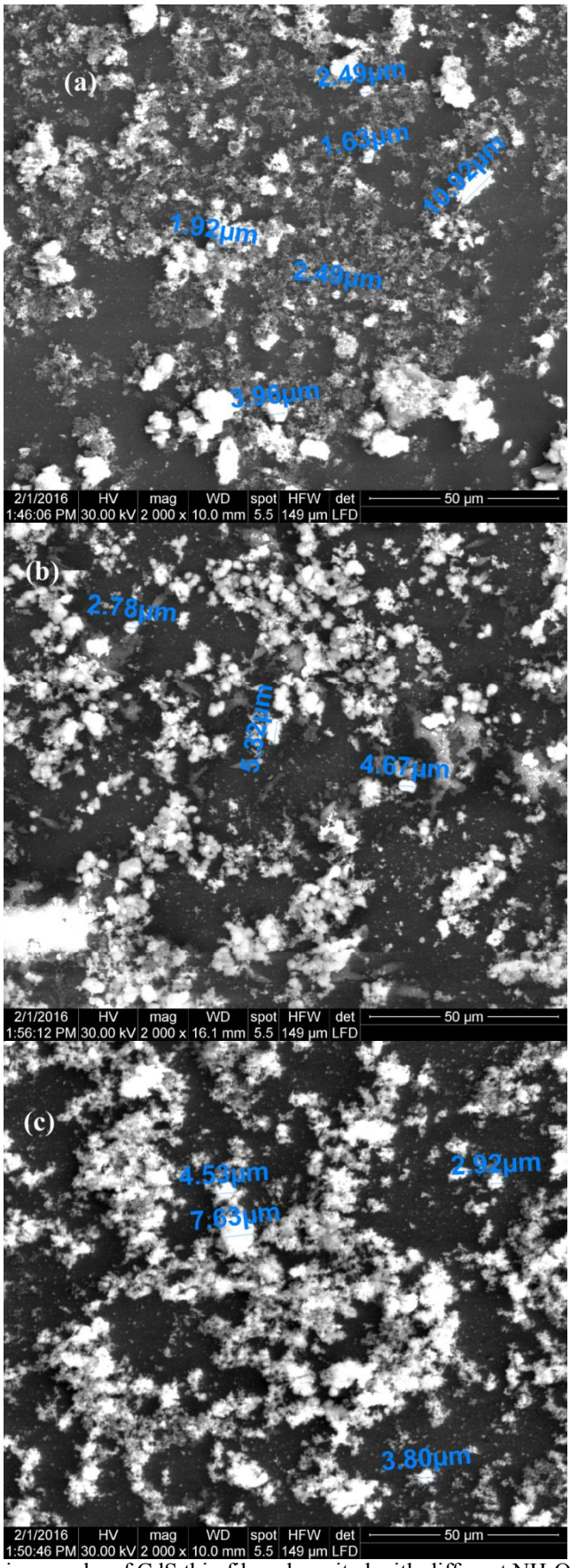


Figure (3) SEM micrographs of CdS thin films deposited with different NH_3OH concentrations: (a)14M ,(b)11M ,(c)8M.

3.1.3 Effect of thiourea concentration

Figure (4) presents the SEM micrographs of the surface morphology of CdS films deposited with different thiourea concentrations (0.06M and 0.09M).It is revealed that increasing of the grain size at high concentration of 0.09M thiourea makes the CdS layer denser and the granules formed a cluster shape with large grains and a few defects, show a good adhesion to the FTO substrate. The EDX analysis for the CdS films prepared with the different thiourea concentrations are summarized as follows. S/Cd ratios are 45.7/54.3and 48.67/51.3 at 0.06M and 0.09M, respectively. Cadmium and sulfur are believed to form the solid solution in the electrolyte and hence the composition of the film is expected to depend on the concentration of chemicals dissolved in the electrolyte. The films are found to be composed of cadmium and sulfur without any foreign impurity. It can be concluded that the film became cadmium-rich with decreasing concentration of thiourea. A satisfactory stoichiometry is achieved for 0.09M of thiourea. A close result was achieved by Chaure et al where they found that this ratio was obtained at 0.13M thiourea [21].

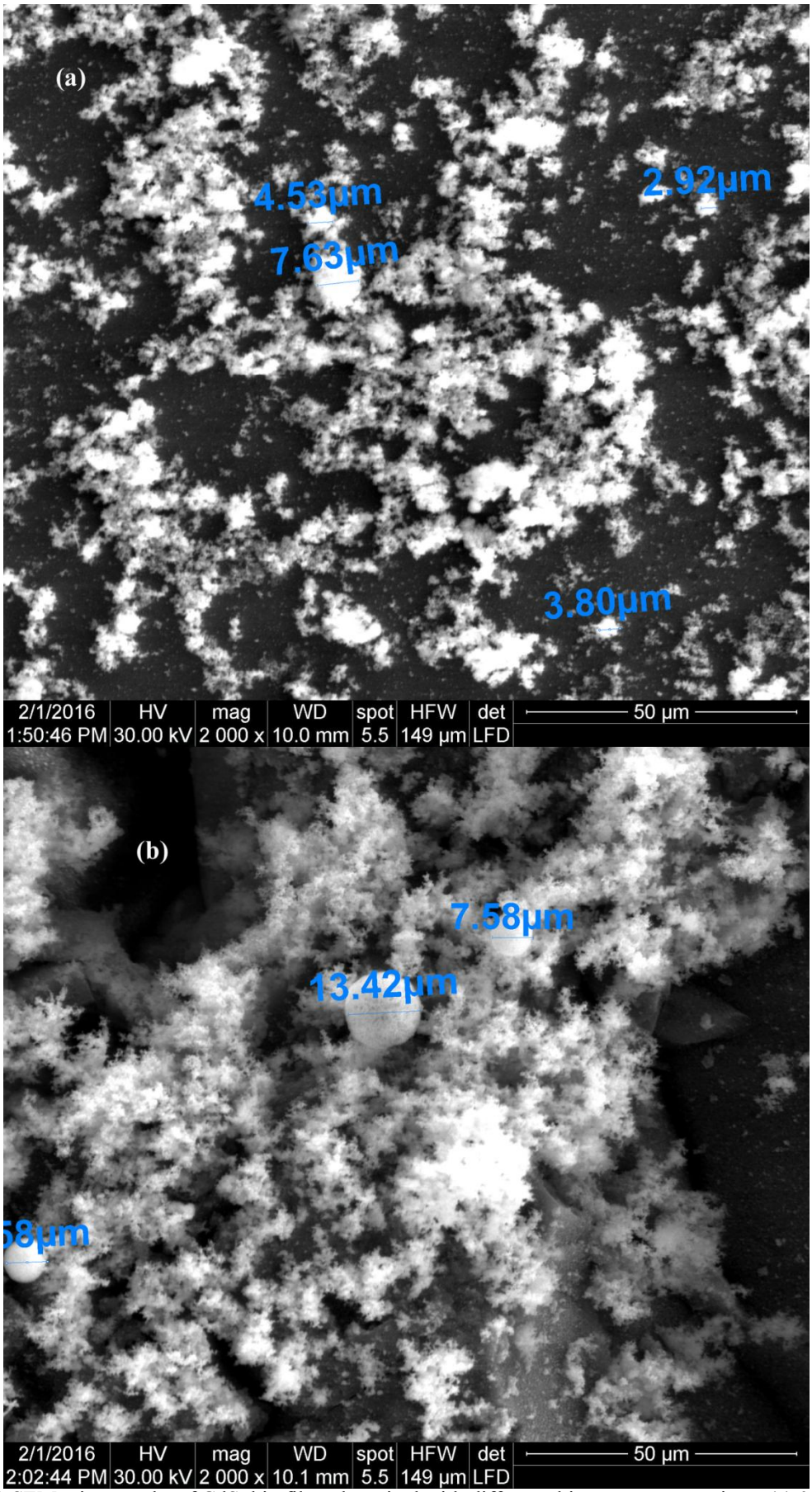


Figure (4) SEM micrographs of CdS thin films deposited with different thiourea concentrations: (a) 0.06M, (b) 0.09M.

3.1.4 Effect of multistage deposition

Figure (5) displays the top surface and cross section SEM micrographs of CdS films deposited with 2 and 6 successive stages. The SEM for the CdS surface deposited with 2 stages has larger porosity and poorer adherence than that obtained with 6 stages due to the multistage deposition process and the produced layer from 6 stages has no cracks. The data available in the literature shows that 2 stages have sponge-like structure with high roughness while the 6 stages we used to deposit CdS film has homogeneous smooth surface. It is observed that the thickness of the CdS layer deposited using 2 and 6 stages are 1.5 and 2.8μm, respectively. The maximum thickness obtained by Mokuralaet al was 100 nm thicknesses within 25 min deposition time using chemical bath deposition and they conclude that increase of thickness with time was linear [22]. Nicholas et al also used CBD and test the deposition time to yield film thicknesses of about 200 nm[23]. Liscoet al compared between pulsed direct current magnetron sputtering and CBD to obtain CdS layer. They found that the deposition rate for CdS obtained using pulsed DC magnetron sputtering was 0.44 nm/s, while the equivalent deposition rate for the CBD was comparatively much slower. To deposit a 50 nm thick film of CdS, about 30min was consumed and a thickness of 150nmneeded 1 h [24]. The EDX analysis shows the S/Cd ratio of 2 and 6 stages CdS films are55.82/44.18 and 51.61/48.39respectively. It is noticed that 6 successive deposition stages is more stoichiometry than 2 deposition stages.

Top surface

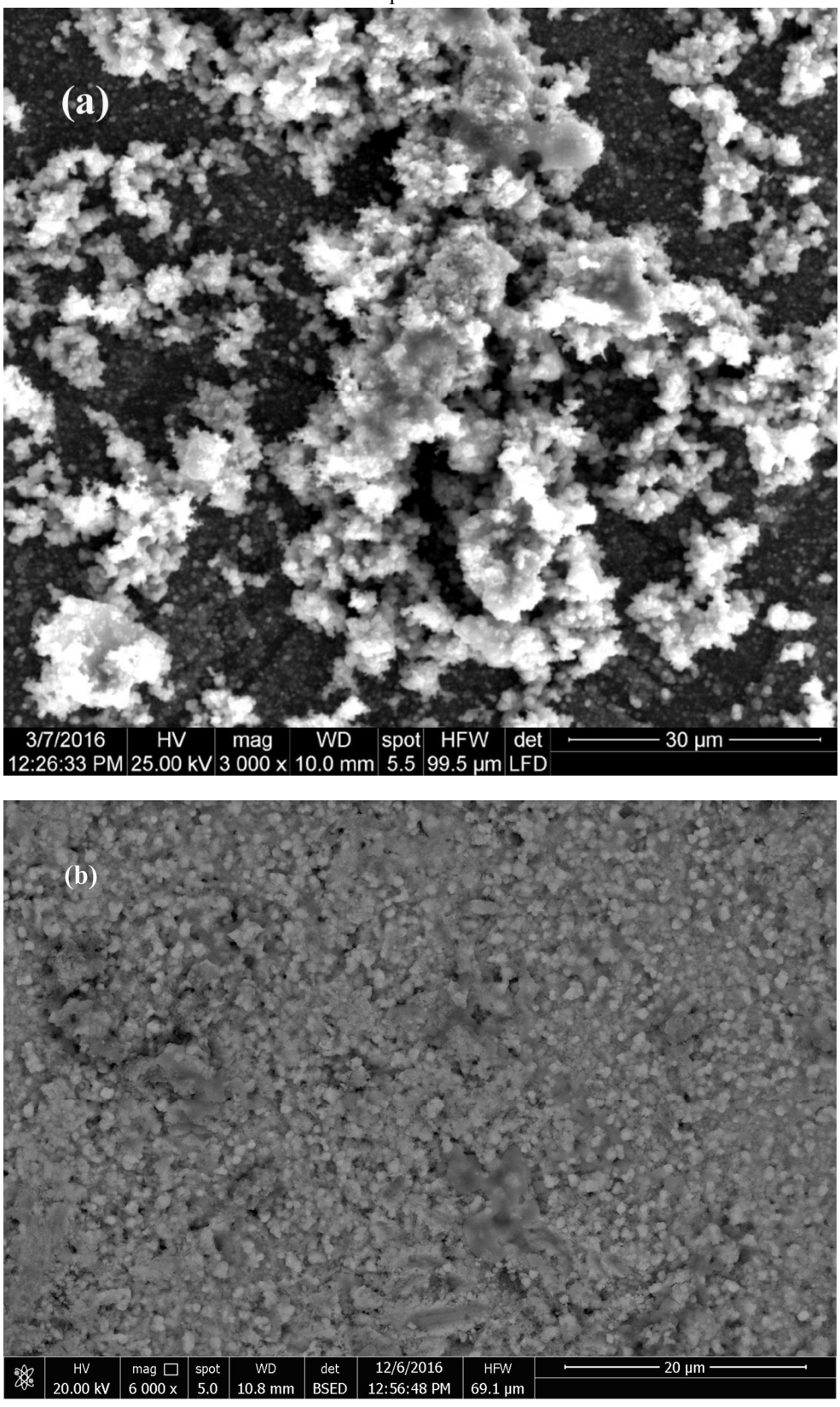
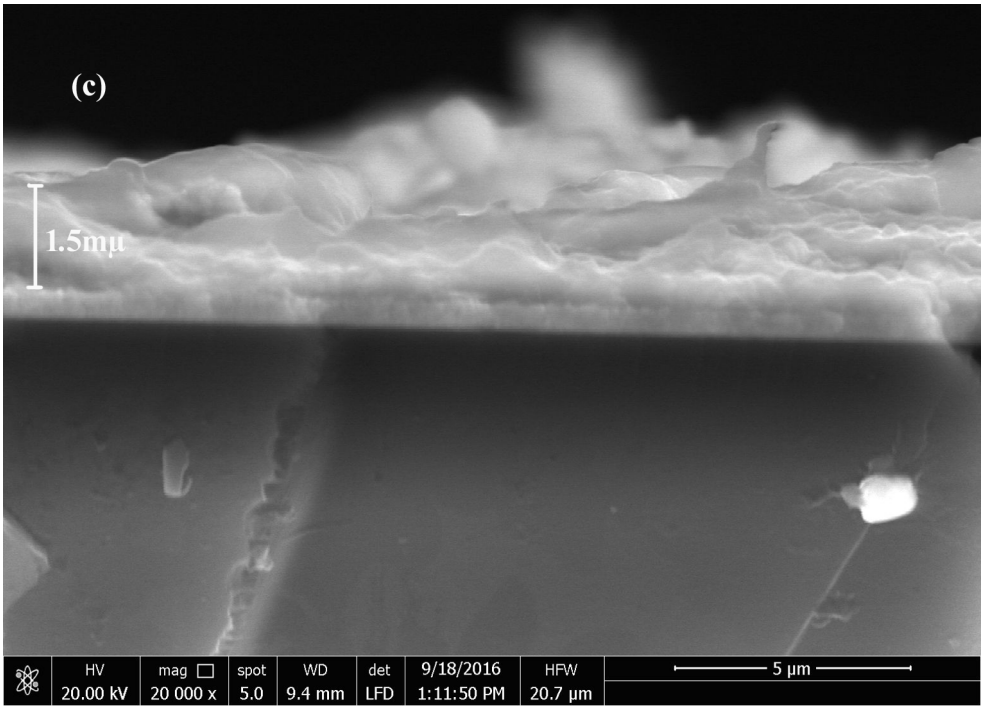


Figure (5) SEM micrographs top surface of CdS films deposited (a) 2 stages, (b) 6 stages

Cross section



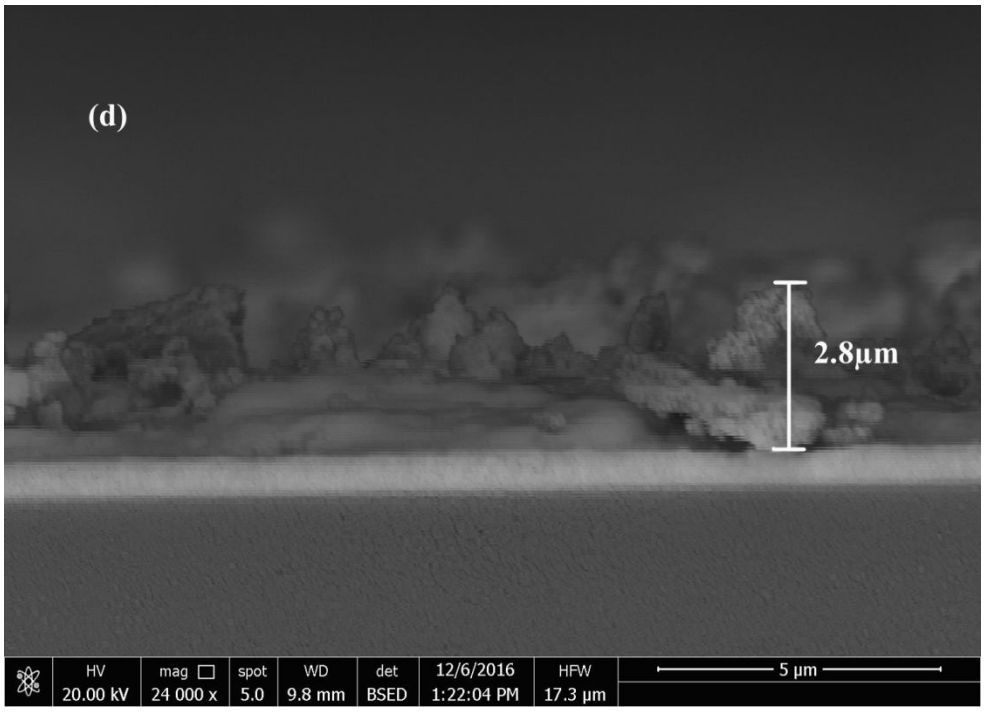


Figure (5) SEM micrographs cross section of CdS films deposited (c) 2 stages, (d) 6 stages

3.2Crystalline structure of CdS thin film

Figure(6)presents the x-ray diffraction patterns of CdS layers deposited with 1,2 and 6 successive stages.The XRD analysis shows that the CdS films have highly oriented crystallites with the classical hexagonal structure (wurtzite type) and the main six diffraction peaks are corresponded to (100), (002), (101), (102), (110) and (103) planes.This is matched with the JCPDS card no. 41-1049 [25]. The intensities of diffracted peaks increase with the rising the number of successive deposition stages. The intensity of the peaks shows that one deposition stage is poorly crystallized, while the intensities of the peaks are improved at 2 deposition stages indicating. If we compare the XRD patterns of CdS film formed with 2 stages with CdS film deposited with 6,we found thatintensity of plane (100) is enhanced by 36%,plane(002) increases by 68%,plane (102) is improved by 32%andthere are no change in intensities of the planes of(110) and (103). It can conclude that preferential orientation of crystallites of CdS film is (002).The relatively stronger and narrow peak of CdS film obtained with 6 stages along (002) plane indicates that the film is highly oriented along the c-axis. This suggests that CdS film deposited with 6 stages of is well crystallized and the increase in intensity of the crystalline peaks with the number of deposition stages is due to the increase of the film thickness[26].

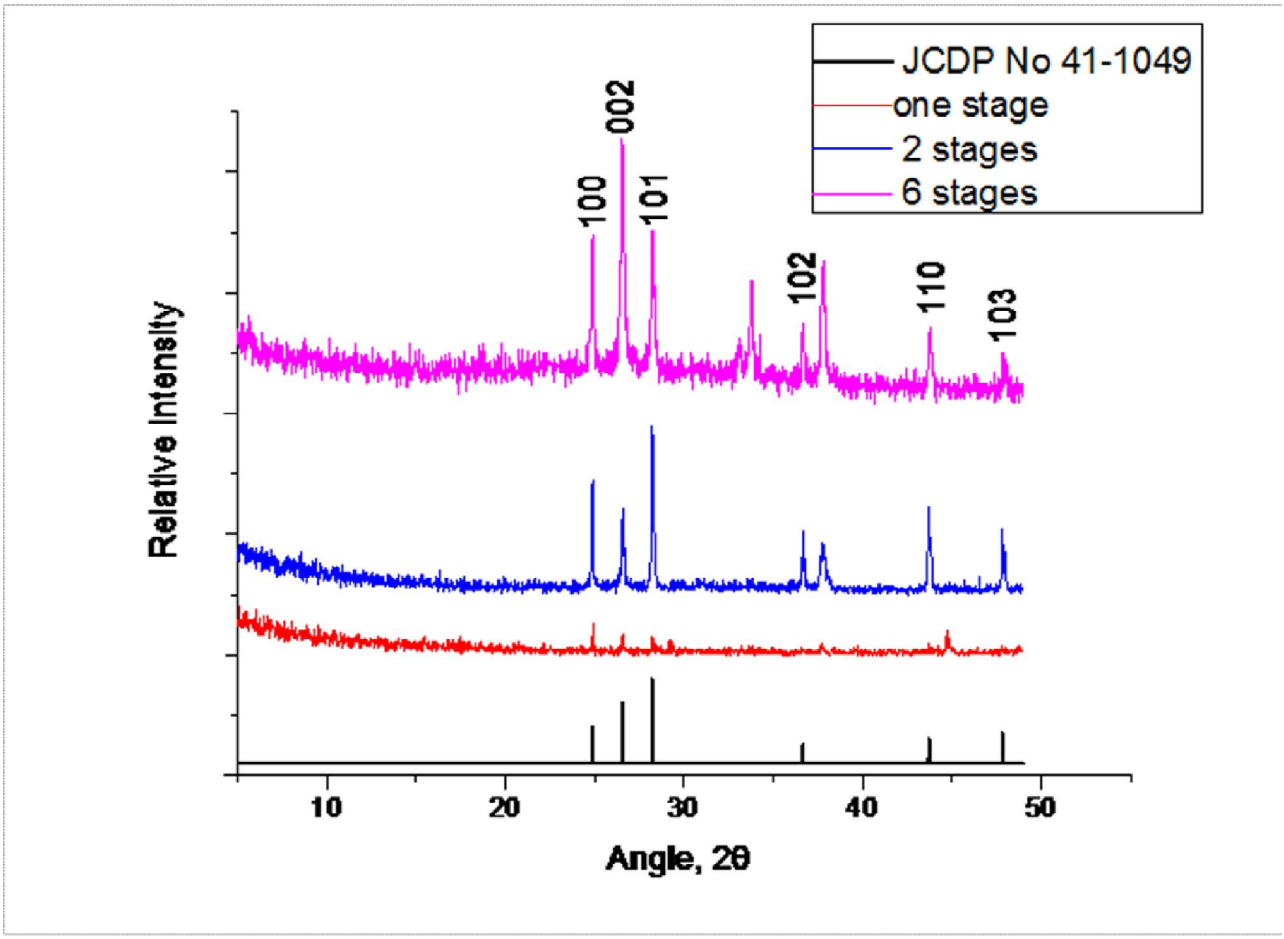


Figure (6) X-ray diffraction patterns of CdS thin films deposited one stage, 2 stages and 6 stages.

3.3 Optical analysis of CdS thin film

The optical transmission spectrum of the CdS film between490 to 720 nm was used toobtain CdS band gap. Figure (7) illustrates the plot of $(\alpha h\nu)^2$ vs. $h\nu$ of the CdS film deposited with one stage. It has been observed that the plot of $(\alpha h\nu)^2$versus$h\nu$ is linear over a wide range of photon energy indicating a specific type of transition. The intercept (extrapolation) of the plot (straight line) on the energy axis reflects the energy band gap. The band gap E_g can be extrapolated to be 2.41 eV. The thickness, refractive index and the absorption coefficientα of thin films calculated by the Swanepoel model, using the following equations [27-28]:

$$n = \left[N + (N^2 + n_s^2)^{1/2}\right]^{1/2} \quad (1)$$

$$N = 2n_s \frac{T_M - T_m}{T_M T_m} + \frac{n_s^2 + 1}{2} \quad (2)$$

$$d = \frac{\lambda_1 \lambda_2}{2(\lambda_1 n_2 - \lambda_2 n_1)} \quad (3)$$

$$\alpha = \frac{1}{d} ln \frac{(n-1)(n-n_s)\left(\frac{T_M}{T_m} + 1\right)^{1/2}}{(n+1)(n+n_s)\left(\frac{T_M}{T_m} - 1\right)^{1/2}} \quad (4)$$

where n is the refraction indices at various wavelengths, T_M and T_m are the maximum and minimum transmissions at specific wavelength λ and n_s is the refractive index of the substrate (n_s=1.52 for glass).n_1 and n_2 are the refractive indices at two adjacent max or min at λ_1 and λ_2, h is Planck constant and υ is the photon's frequency. The calculated average thickness, and refractive index were 0.91 μm, and 2.46 respectively.

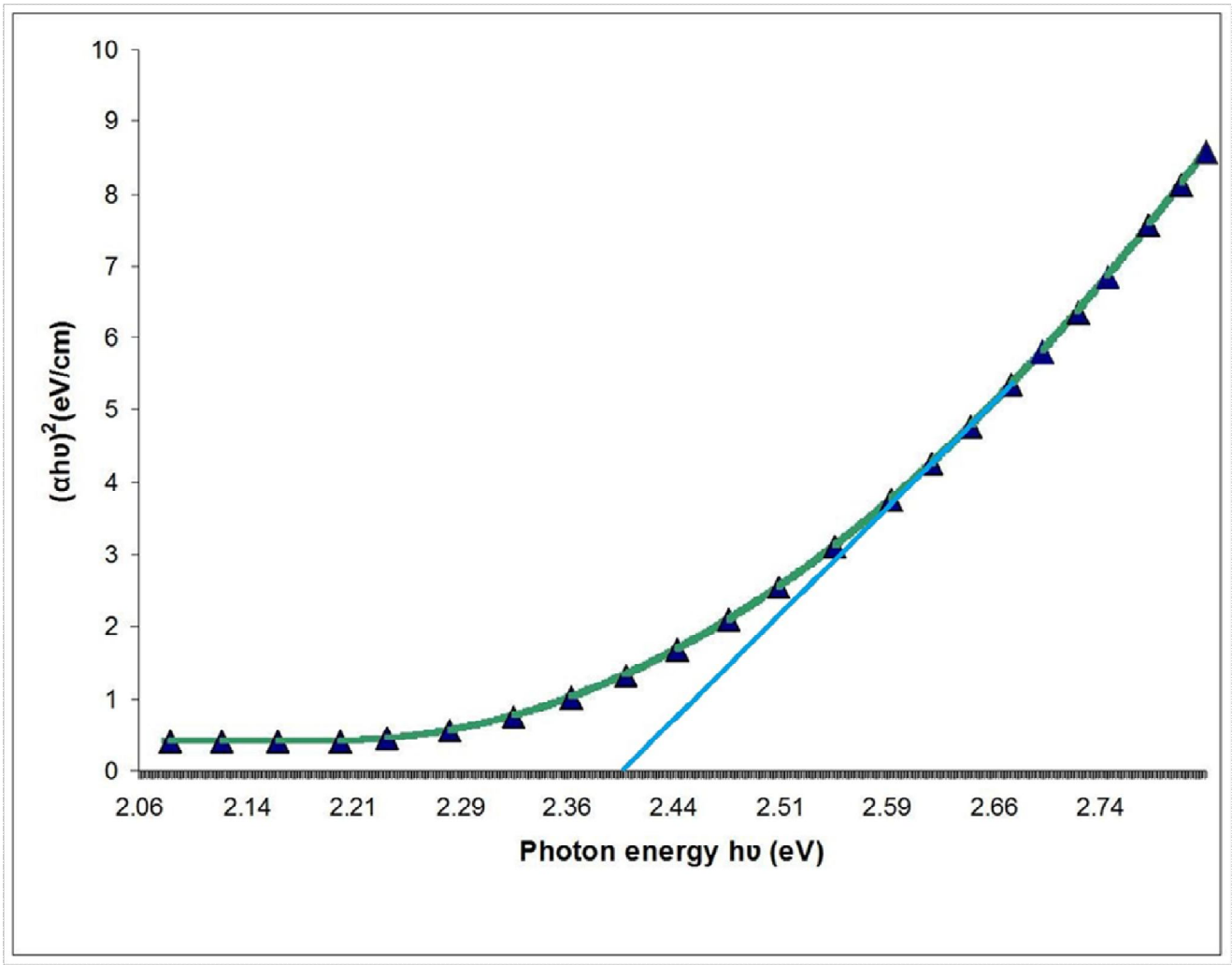


Figure (7) $(\alpha h\upsilon)^2$ versus $h\upsilon$ of CdS deposited film using one stage method.

3.4 Performance of FTO/CdS/CdTe/Mo X-ray detector

Figure (8a) shows output signal from FTO/CdS/CdTe/Mo detector exposed to x-ray of 33 keV and 1mA intensity. It is observed that the maximum and the minimum amplitudes of the pulse formed due to exposed FTO/CdS/CdTe/Mo detector to X-ray of 33 keV and 1mA intensity are 0.732 and -0.405 V and consequently the total signal amplitude is 1.137 V. If R represents the input resistance of the circuit and C represents the equivalent capacitance of both the FTO/CdS/CdTe/Mo detector and the measuring circuit. The time-dependent voltage V(t) across the load resistance is the fundamental signal voltage output the pulses which their amplitudes depend on the amount collected charges and relative value of the time constant of the measuring circuit. The time constant equals to RC. If the time between pulses is sufficiently large, the capacitance will discharge through the resistance and the voltage across the load resistance returns to zero. So the time required for the signal pulse to reach its maximum value is determined by the charge collection time within the FTO/CdS/CdTe/Mo detector. The time required to restore the signal voltage to zero is determined by the time constant of the load circuit. The amplitude of the signal pulse is determined by the ratio of the total charge created within the detector during one radiation interaction divided by the capacitance of the equivalent load circuit. Because the capacitance is fixed, the amplitude of the signal pulse is directly proportional to the generated charge [29]. The signal formation is through three steps. In step (1), is the formation of depletion region or junction prevents the passing of the free charges from the bulk. In step (2), X-ray passes through the FTO/CdS/CdTe/Mo detector where the most interaction occurred in the CdS/CdTe junction. X-ray photons are disappeared and a photoelectron produced from one of the electron shells of the absorber CdS/CdTe junction with kinetic energy equals the incident photon energy minus the binding energy of the electron in its original shell. The vacancy that is created in the electron shell as a result of the photoelectron emission is quickly filled by electron rearrangement where a characteristic X-ray is produced. X-rays reabsorbed again through photoelectric interactions with less tightly bound electron shells of the CdS/CdTe junction. In step (3), the produced electrons cause the appearance of a given amount of electric charge within the detector. These created charges flow in the opposite directions and collected at the electrodes causing electrical pulses.

Figure (8b) shows the output signal of FTO/CdS/CdTe/Mo detector versus X-ray energy at different intensities. The amplitude is linearly increased with energy of X-ray until 33 keV then there is a very slight increase in the signal amplitude. The electron-hole pairs produced from high energy X-ray are far from the junction of the detector and consequently the recombination process of electron-hole pairs is dominant. We can conclude that the linearity of the FTO/CdS/CdTe/Mo detector is better at lower intensity of X-ray than obtained at higher intensity [30]. Shin Watanabe developed two prototype models of the CdTe stacked detector which consists of 10 and 40

CdTe detectors. Each diode has an area of 21.5 mm × 21.5 mm and a thickness of 0.5 mm. A bias voltage of 300 V was used. The 10 layer module was used to measure the spectrum of ^{60}Co which radiate gamma ray with energy 1173 keV and 1332 keV. The 40 layer module used to measure the higher energy source ^{252}Cf which produce neutrons with energy 5100, 5600 and 6100 keV. The idea of plural planer detectors with the high thickness of detector increased the probability of interaction which make the detector can detect gamma ray and neutron in the energy range from 1.17 to 5.6 MeV [31]. In our work we used the energy range from 21 to 42 keV because the maximum obtained thickness for CdS/CdTe junction is 6.8 μm. The stacked 4 CdS/CdTe junction increases the area of the detector. As the area increases, the number of interactions of X-ray with CdS/CdTe junction increases and the collected charge and the amplitude of signal increase.

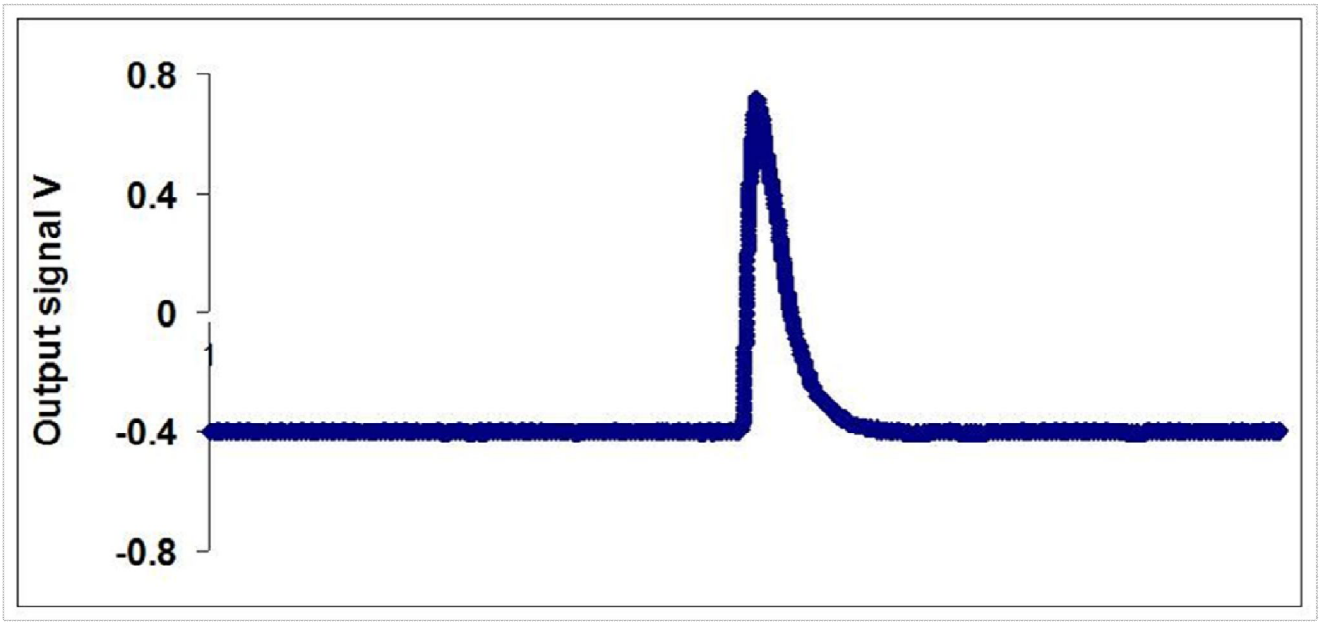


Figure (8a) Output signal of FTO/CdS/CdTe/Mo detector exposed to x-ray of 33 keV and 1mA intensity

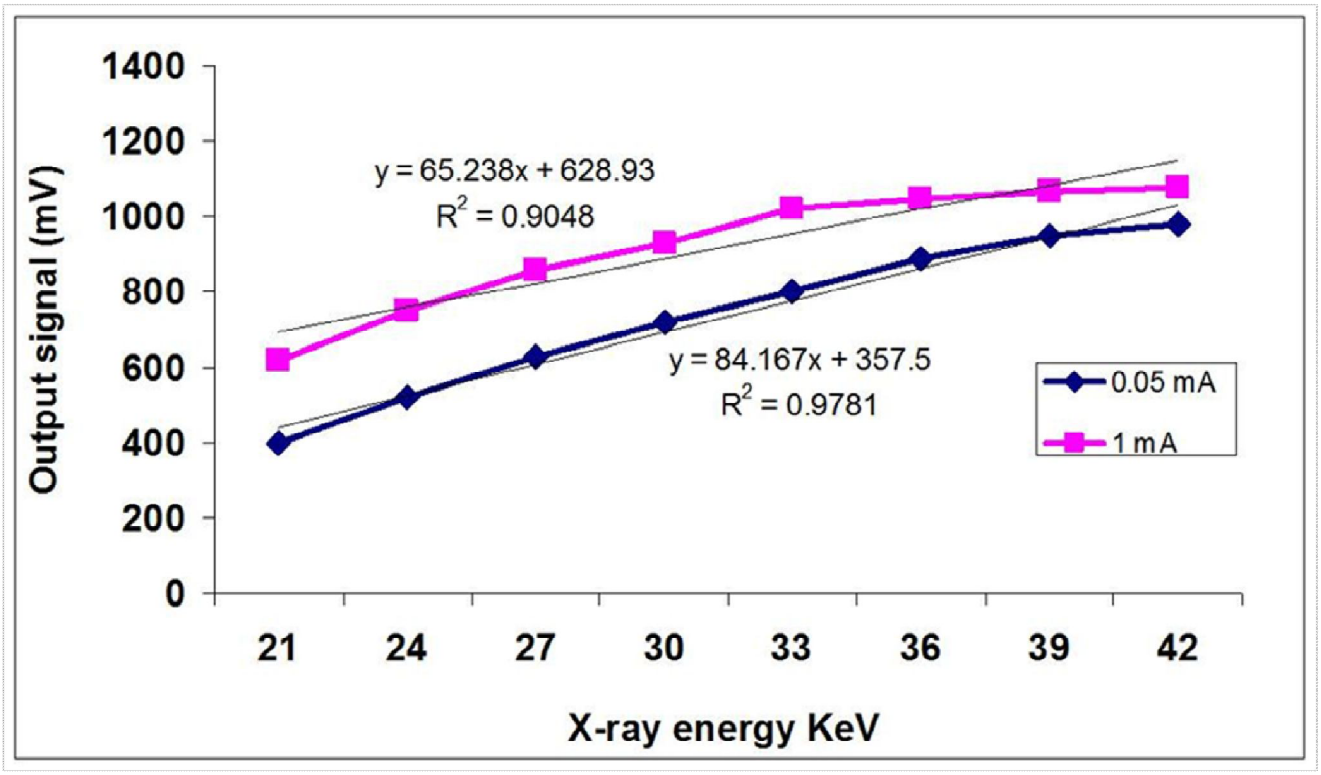


Figure (8b) output signal of FTO/CdS/CdTe/Mo detector versus x-ray energy at different intensities

4. Conclusion

Multilayer of CdS using CBD were succeeded to deposit thick layer to fabricate FTO/CdS/CdTe/Mo X-ray detector. The optimal concentrations were found to be 0.09 M and 8 M for thiourea and ammonia, respectively, while the optimum deposition time was 4 hours with 1 N $CdCl_2$ with heat treatment at 350^{o}C for 15 min. These optimal deposition parameters were used to produce thick film by depositing 6 successive thin films. The side view SEM indicated that 6 stages deposition of CdS layers yielded 2.8 μm. The performance of the FTO/CdS/CdTe/Mo X-ray detector produced electric pulse and the maximum and the minimum amplitudes of this pulse were 0.732 and -0.405 V at33 keV and 1mA.

References

[1] R.S. Mane, and C.D. Lokhande, Materials Chemistry and Physics I-31, 65 (2000)

[2] H. Khallaf , Isaiah O. Oladeji, G. Chai, and L. Chow, Thin Solid Films 7306–7312, 516 (2008).

[3] S. Wagner, J. L. Shay, P. Migliorato, and H. M. Kasper, (1974) https://doi. 10.1063/1.1655537

[4] Y. Tomita, Y. Hatanaka, T. Takabayashi, and T. Kawai (1993) https://doi. 10.1109/16.182507

[5] J. W. Murphy, J. W., L. Smith, J. Calkins, and G. R. Kunnen, (2014). https://doi.org/10.1063/1.4895925.

[6] J. Kang, E. I. Parsai, D. Albin, V. G. Karpov, and Diana Shvydka. (2008) https://doi: 10.1063/1.3042212.

[7] M Ilieva, D. Dimova Malinovska, B. Ranguelov and I Markov, Condens. Matter 10025–10031, 11 (1999).

[8] A. Palafox, G. R. Paredes, A. Maldonado, R. Asomoza, D.R. Acosta, and J. Palacios-Gomez, Solar energy Materials and Solar Cells. 31-41, 55 (1998).

[9] P. Boieriu, R. Sporken, Y. Xin, N.D. Browning, and S. Sivananthan, (1999) https://doi. 10.1007/s11664-000-0212-3.

[10] H. Uda, H. Yonezawa, Y. Ohtsubo, M. Kosaka, and H. Sonomura, Solar Energy Materials and Solar Cells 219–226, 75 (2003).

[11] M. Sasagawa, and Y. Nosaka, Electrochimica Acta 483-488, 48 (2003).

[12] B. E. Mcandless, I. Youm, and R. W. Birkmire, (1999) https://doi: 10.1002/(SICI)1099-159X(199901/02)7:1<21::AID -PIP244>3.0.CO;2-D.

[13] M.A. Islam, M.S. Hossain, M.M. Aliyu, P. Chelvanathan, Q. Huda,M.R. Karim, K. Sopian, and N. Amin, Energy procedia 203 – 213, 33 (2013).

[14] S. Ramprasad, Y. Su, C. Chang, B. K. Paul, D. R. Palo; Solar Energy Materials and Solar Cells 77–85, 96 (2012).

[15] I. O. Oladej, and L. Chow, (1997) https://doi: 10.1149/1.1837815

[16] D. H. Rose and F. S. , Photovolt: Res. Appl., 331-340, 7 (1999).

[17] F. Ouachtari, A. Rmili, S. El Bachir, A. Bouaoud, H. Erguig, and P. Elies, Modern Physics, 1073-1082, 2 (2011).

[18] M. Reddy, and N. Vara, IOSR Applied Physics 2278-4861, 4 (2013).

[19] A. Hasnat and J. Podder, Bangladesh Academy of Sciences, 33-41, 1 (2013).

[20] R. J. Xavier, A. J. Amalraj, and V. Dharmalingam, Chem. Tech. Research, 0974-4290, 3 (2017)

[21] S. Chaure, N.B. Chaure, R.K. Pandey and A.K. Ray, (2007) https://doi:10.1049/iet-cds:20070048.

[22] K. Mokurala, L. L. Baranowski, F. Willian, S. Siol, M. Van Hest, S. Mallick, P. Bhargava, and A. Zakutayev, (2016) https://doi: 10.1021/acscombsci.6b00074.

[23] J. N. Alexander, S. Higashiya, D. Caskey, H. Efstathiadis, and P. Haldar, (2014) https://doi.org/10.1016/j.solmat. 2014.02.017

[24] F. Lisco P.M. Kaminski, A. Abbas , K. Bass, J.W. Bowers, G. Claudio, M. Losurdo, J.M.Walls, (2014) https://doi.org/10.1016/j.tsf.2014.11.062.

[25] Weizhi Wang, Yajing Lu, Yafei Xu, Konglin Wu, Jiarui Huang, Changchun Jia and Si Ok Ryu, Royal society journal of chemistry, (2016) https://doi: 10.1039/c6ce00025h.

[26] A. Nawaz, Z. Rabeel and N. A. Shah, (2014) https:// doi: 10.5829/idosi.wasj.2014.31.08.621.

[27] J. C. Manifacier, J. Gasiot and J. P. Fillard, (1976) https://doi: 10.1088/0022-3735/9/11/032.

[28] S. ilican, M. Caglar, and Y. Caglar, Material Science-Poland, 0137-1339, 3 (2007).

[29] G. E. Knoll. Radiation Detection and Measurement 3rd edn., (John Wiley and Sons, New York, 2000) (PP. 48:53, 103:111, 308:317)

[30] J. Abramovitch, Engaged learning at SMUD digital repository, (2014), http://digitalrepository.smu.edu/upjournal_research/32.

[31] S. Watanabe, T. Takahashi, K. Nakazawa, Y. Kobayashi, Y. Kuroda, K. Genba, M. Onishi, and K. Otake, (2003) https://doi: org/10.1016/S0168-9002(03)01032-5.